1 Constant η

1.1 Toy Problem

Consider simplest spin Hamiltonian $H = -\vec{B}\cdot\vec{s}$. It's clear that if we set up initial conditions $\vec{s}$ misaligned from $\vec{B}$, it will simply spin around $\vec{B}$, which is fixed. Thus, let $\hat{B}\cdot\hat{s} = \cos\theta$ the angle between the two, and let ϕ measure the azimuthal angle.

We claim that $\cos\theta, \phi$ are canonical variables. Since ϕ is ignorable, immediately $\frac{\mathrm{d}\theta}{\mathrm{d}t} = \frac{\mathrm{d}\cos\theta}{\mathrm{d}t} = -\frac{\partial H}{\partial\phi} = 0$, while $\frac{\mathrm{d}\phi}{\mathrm{d}t} = \frac{\partial H}{\partial(\cos\theta)} = Bs$ tells us the rate at which the spin precesses around $\vec{B}$.

1.2 Cassini State Hamiltonian

This Hamiltonian is Kassandras Eq. 13, in the co-rotating frame with the perturber's angular momentum:

$$\mathscr{H} = \frac{1}{2}\big(\hat{s}\cdot\hat{l}\big)^2 - \eta\big(\hat{s}\cdot\hat{l}_p\big). \tag{1}$$

In this frame, we can choose $\hat{l} \equiv \hat{z}$ fixed, and $\hat{l}_p = \cos I\hat{z} + \sin I\hat{x}$ fixed as well. Then

$$\hat{s} = \cos\theta\hat{z} - \sin\theta\big(\sin\phi\hat{y} + \cos\phi\hat{x}\big).$$

We can choose the convention for $\phi = \phi$ azimuthal angle requiring $\phi = 0, \pi$ mean coplanarity between $\hat{s}, \hat{l}, \hat{l}_p$ in the $\hat{x}, \hat{z}$ plane such that $\hat{l}_p, \hat{s}$ lie on the same side of $\hat{l}$. Then we can evaluate in coordinates

$$\begin{aligned}
\hat{s}\cdot\hat{l} &= \cos\theta, \\
\hat{s}\cdot\hat{l}_p &= \cos\theta\cos I - \sin I\sin\theta\cos\phi, \\
\mathscr{H} &= -\frac{1}{2}\cos^2\theta + \eta\big(\cos\theta\cos I - \sin I\sin\theta\cos\phi\big).
\end{aligned}$$

Note that if we take $\cos\theta$ to be our canonical variable, $\sin\theta = \sqrt{1-\cos^2\theta}$ can be used.

1.3 Equation of Motion

The correct EOM comes from Kassandra's Eq. 12:

$$\begin{aligned}
\frac{\mathrm{d}\hat{s}}{\mathrm{d}t} &= \big(\hat{s}\cdot\hat{l}\big)\big(\hat{s}\times\hat{l}\big) - \eta\big(\hat{s}\times\hat{l}_p\big), \\
&= \big(s_y s_z - \eta s_y\cos(I)\big)\hat{x} - \big(s_x s_z + \eta(s_x\cos I - s_z\sin I)\big)\hat{y} + \eta s_y\sin(I)\hat{z}.
\end{aligned}$$

Alternatively, consider Hamilton's equations applied to the Hamiltonian:

$$\frac{\partial\phi}{\partial t} = \frac{\partial\mathscr{H}}{\partial(\cos\theta)} = -\cos\theta + \eta\big(\cos I + \sin I\cot\theta\cos\phi\big), \tag{2}$$

$$\frac{\partial(\cos\theta)}{\partial t} = -\frac{\partial\mathscr{H}}{\partial\phi} = -\eta\sin I\sin\theta\sin\phi. \tag{3}$$

This produces the same trajectories as the Cartesian EOM, so this is correct. However, since $\frac{\partial\phi}{\partial t} \propto 1/\sin\theta$, this is not a desirable system of equations to use, as they are very stiff near $\theta \approx 0$.

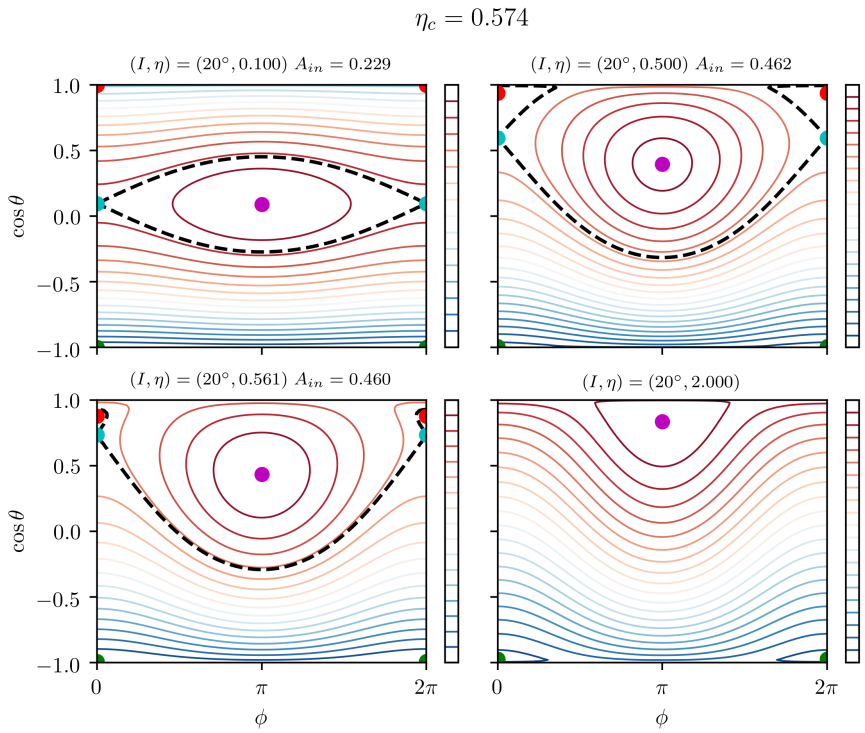

Figure 1: Separatrix for various values of η.

1.4 Cassini States

The zeros to Eq. 3 are the Cassini states; we will go to canonical variables $\mu = \cos\theta$. We can immediately see that $\sin\phi = 0$ is necessary, so $\cos\phi = \pm 1$ and we need only solve for $\frac{\partial\phi}{\partial t} = 0$. We can furthermore separate the problem into two regimes, $\eta \ll 1$ and $\eta \gg 1$.

For $\eta \ll 1$, it is clear that there will be two solutions near $\mu^2 = 1$ and two solutions near $\mu = 0$:

- For $\mu = 1 - \frac{\theta^2}{2}$, the dominant terms are $\frac{\partial\phi}{\partial t} \approx -1 + \eta\sin I\frac{1}{\theta} = 0$, where we've taken $\cos\phi = +1$ and $\phi = 0$. This forces $\theta = \eta\sin I$.
- Similarly, for $\mu = -1 + \frac{\epsilon^2}{2}$, $\phi = 0$ and $\epsilon = \eta\sin I$ again. This actually corresponds to $\theta = \pi - \eta\sin I$.
- For $\mu \approx 0$, we have instead $\frac{\partial\phi}{\partial t} = -\mu\big(1 - \eta\sin I\cos\phi\big) + \eta\cos I = 0$. This forces $\mu_\pm = \frac{\eta\cos I}{1\pm\eta\sin I}$, where $\phi_\pm = \pi, 0$ respectively.

  Note that $\phi = 0, \mu \approx 0$ is conventionally CS4. The linearization locally has form $\frac{\partial\delta\phi}{\partial t} = -\delta\mu\big(1 - \eta\sin I\big)$ and $\frac{\partial\delta\mu}{\partial t} = -\eta\sin I\delta\phi$, so the eigenvalues are $\approx \mp\sqrt{\eta\sin I}$, and the two eigenvectors are $\big(1, \pm\sqrt{\eta\sin I}\big)$.

For $\eta \gg 1$, the solutions obviously just come from $\cos I \pm \sin I\cot\theta = 0$, which are just $\sin(I \pm \theta) = 0$

1.5 Separatrix Area

We can estimate the area enclosed by the separatrix, as shown in Fig. 1. Note that the separatrix joins Cassini State 4 to its $+2\pi$ image.

We notate $\mu = \cos\theta$; note that CS4 is $\mu_4 \approx \frac{\eta\cos I}{1-\eta\sin I} \approx \eta\cos I$. Setting the Hamiltonian equal to its value at CS4 gives

$$\begin{aligned}
H_4 \equiv H(\mu_4,\phi_4) &\approx -\frac{\mu_4^2}{2} + \eta\mu_4\cos I - \eta\sin I,\\
&= +\eta^2\cos^2 I - \eta\sin I,\\
H(\mu_{sep},\phi_{sep}) = H_4 &= -\eta\sin I\cos\phi_{sep} - \frac{\mu_{sep}^2}{2} + \eta\mu_{sep}\cos I + \mathcal{O}(\eta^3),\\
0 &\approx \frac{\mu_{sep}^2}{2} - \eta\mu_{sep}\cos I - \eta\sin I\left(1-\cos\phi_{sep}\right) + \eta^2\cos^2 I,\\
\mu_{sep}(\phi) &\approx \sqrt{2\eta\sin I\left(1-\cos\phi\right)} + \mathcal{O}(\eta).
\end{aligned}$$

We can then easily compute the area enclosed by the separatrix

$$\begin{aligned}
A_{sep} &= \int_0^{2\pi} 2\mu_{sep}\,\mathrm{d}\phi,\\
&\approx 16\sqrt{\eta\sin I}.
\end{aligned} \tag{4}$$

For $\eta = 0.1, I = 20^\circ$, this predicts $\frac{A_{sep}}{A_T} \approx 0.235$, which is pretty close to my numerically calculated $\frac{A_{sep}}{A_T} = 0.229$.

2 Separatrix Hopping

Inspired by G&H, heteroclinic orbits are topologically unstable for any nonzero perturbation, but opened width ~ perturbation parameter. Thus, if we introduce a small and constant tidal dissipation, we should get a *asymptotically constant* probability of hopping the separatrix.

2.1 Tidal Dissipation

We can add a tidal dissipation term; we write it in form $\left(\frac{\mathrm{d}\hat{s}}{\mathrm{d}t}\right)_{tide} = \epsilon\hat{s}\times\left(\hat{l}\times\hat{s}\right) = \epsilon\left(\vec{l} - \left(\vec{s}\cdot\vec{l}\right)\vec{s}\right)$. Expanding,

$$\begin{aligned}
\left(\frac{\mathrm{d}\hat{s}}{\mathrm{d}t}\right)_{tide} &= \epsilon(\hat{z} - s_z\hat{s}),\\
&= \epsilon\left(-s_z s_x\hat{x} - s_z s_y\hat{y} + \left(1-s_z^2\right)\hat{z}\right).
\end{aligned} \tag{5}$$

We run numerical simulations for weaker $\epsilon \ll \eta \ll 1$ and stronger $\epsilon \lesssim \eta \ll 1$.

We can seek equilibria of the the system including tides, which requires

$$\begin{aligned}
0 &= s_y s_z - \eta s_y\cos I - \epsilon s_z s_x,\\
0 &= -s_x s_z - \eta(s_x\cos I - s_z\sin I) - \epsilon s_z s_y,\\
0 &= \eta s_y\sin(I) + \epsilon\left(1-s_z^2\right).
\end{aligned}$$

We expect at least two equilibria, based on the simulations: one near $s_z \approx 1$ and one $s_z \approx 0$.

For near alignment/near Cassini state 1, $1 - s_z \sim 1 - s_\perp^2$, so we can set $s_z = 1$ to first order: $s_y - \epsilon s_x - \eta s_y\cos I = -s_x - \eta(s_x\cos I - \sin I) - \epsilon s_y = \eta s_y\sin I = 0$. This can be satisfied if we set $s_x = \tan(I) \ll 1, s_y = \mathcal{O}(\epsilon s_x)$; this coarsely corresponds to Cassini state 1.

The other solution should be near Cassini state 2, where $s_x \approx 1$; dropping second order terms forces $\eta s_y + \epsilon s_z = -s_z - \eta(\cos I - s_z \sin I) = \eta s_y \sin(I) + \epsilon = 0$. This can thus be satisfied for $s_y \approx -\frac{\epsilon}{\eta \sin(I)}$. Thus, this explains why as ϵ is increased, we first start to get points that don't converge to Cassini state 2 in the absence of tides, before starting to see points that fail to converge to Cassini state 1.

2.2 Consideration 1: Qualitative

We zoom in on Cassini State 4, which has $\theta_4 = -\frac{\pi}{2} + \frac{\eta \cos I}{1-\eta \sin I}, \mu_4 = \frac{\eta \cos I}{1-\eta \sin I}, \phi_4 = 0$. Then, using equations of motion

$$\frac{\partial \phi}{\partial t} = \mu - \eta\left(\cos I + \sin I \frac{\mu}{\sqrt{1-\mu^2}} \cos\phi\right), \tag{6}$$

$$\frac{\partial \mu}{\partial t} = -\eta \sin I \sin\phi + \left[\epsilon\left(1-\mu^2\right)\right], \tag{7}$$

we can perturbatively require $\frac{\partial \theta}{\partial t} = 0$ for $\epsilon \neq 0$. This corresponds to $\eta \sin I \sin\left(\phi_4 + \delta\phi\right) \approx \epsilon$, or $\delta\phi_4 = +\frac{\epsilon}{\eta \sin I}$. This is in agreement with Dong's result.

This implies that the stable manifolds of the two saddle points, which once overlapped with each other's unstable manifolds (creating a heteroclinic orbit) now are offset from one another by distance $D \sim \frac{\epsilon}{\eta \sin I}$. But since ϵ also sets $\dot{\mu}$ in a precession orbit-averaged sense, the effective cross section is constant in some sense: there will be one orbit where μ goes from below CS4 to above CS4, during which it will make jump of size ϵ, and if it hits a particular interval of size ϵ then it will enter the separatrix. Thus, separatrix hopping should $\propto \epsilon^0$.

2.3 Consideration 2: Melnikov Distance

We notice that the separatrix is a heteroclinic orbit, or a saddle connection, in the dissipation free problem. Introducing dissipation breaks the saddle connection by a distance that can be estimated with the Melnikov distance. This is G&H Equation 4.5.11 or something:

$$d(t_0) = \frac{\epsilon M(t_0)}{\left|f(q^0(0))\right|} + \mathcal{O}(\epsilon^2), \tag{8}$$

$$M(t_0) = \int_{-\infty}^{\infty} [f \times g]_{hetero} \, \mathrm{d}t. \tag{9}$$

This is not a hard formula to understand; along the separatrix, motion is dominated by f, but the perpendicular component adds up to contribute to a total "perpendicular distance away from the original separatrix" necessary to hit the saddle point, at least intuitively.

We evaluate the Melnikov integral $M(t_0)$ on the heteroclinic orbit. Note that since in our problem our perturbation g is time-independent, so too is the Melnikov integral $M(t_0) = M$.

Let's apply this to the Cassini state Hamiltonian w/ dissipation. We first write down our EOM in Melnikov form (we use canonical variables μ, ϕ):

$$\frac{\mathrm{d}\hat{s}}{\mathrm{d}t} = \underbrace{\frac{\partial \mathcal{H}}{\partial \mu}\hat{\phi} - \frac{\partial \mathcal{H}}{\partial \phi}\hat{\mu}}_{f} + \epsilon \underbrace{\left(1-\mu^2\right)\hat{\mu}}_{g}. \tag{10}$$

Then $f \times g = f_\phi g_\mu = \frac{\partial \mathcal{H}}{\partial \mu}\left(1-\mu^2\right)$. We then want to integrate this along the heteroclinic orbit. We can make change of variables

$$M = \int_0^{2\pi} \frac{\partial \mathcal{H}}{\partial \mu}\left(1-\mu^2\right)\left(\frac{\partial \phi}{\partial t}\right)^{-1} \mathrm{d}\phi. \tag{11}$$

But thankfully, $\frac{\partial \mathscr{H}}{\partial \mu} = \frac{\partial \phi}{\partial t}$ in the absence of dissipation, and so $M = 2\pi\left(1-\mu^2\right) \approx 2\pi$. Thus, the Melnikov distance at point q^0, a point on the heteroclinic orbit of the unperturbed Hamiltonian, is just

$$d(q^0) = \frac{2\pi\epsilon}{\left|f(q^0)\right|}. \tag{12}$$

Note that the maximum value $\left|f(q^0)\right|$, which occurs at $\phi = \pi$, is just $f_{\max} \approx \sqrt{4\eta \sin I}$.

It proves to be a bit difficult to make quantitative predictions though, since the phase diagram is very smushed where f is large, and d is rather inaccurate where f is small. Let's think about a Poincaré map instead.

2.4 Consideration 3: Poincaré Section

Let's consider the Poincaré section every time $\phi = \phi_4$ as the trajectory subject to tidal dissipation is moving $\theta < \theta_4 \to \theta_4$. To provide an estimate of $\Delta\theta(\theta) = \theta_{n-1} - \theta_n$, this is just ϵT where T is the time elapsed between θ_n, θ_{n+1}, the period of the orbit. T is dominated by when $\frac{\partial \phi}{\partial t} \ll 1$ though, or where the orbit is close to the saddle point.

Note that T is dominated by the time it spends near the saddle point. We showed earlier that near CS4, $\frac{\partial \phi}{\partial t} \approx \delta\mu$ where $\delta\mu = \mu - \mu_4$. Thus, we might surmise $\Delta\theta(\theta) \propto \theta^{-1}$ for sufficiently small $\theta - \theta_4$. Far away, T is roughly constant and $\Delta\theta(\theta)$ is roughly constant.

What is "far away"? Well, it probably depends on how affected our trajectory is by the separatrix; far away from the saddle point, we go along contours of roughly constant θ, while close by we follow the separatrix pretty well. We computed earlier that $\mu_{sep} \sim \sqrt{4\eta \sin I}$, so we might expect $\mu > \mu_{sep}, \Delta\mu \sim C$, while $\mu < \mu_{sep}, \Delta\mu \sim \delta\mu^{-1}$.

My $\mu > \mu_{sep}$ simulations don't seem to work very well, so I'll focus on the $\delta\mu^{-1}$ case. In this case, define $\delta\mu_c : \Delta\mu\left(\delta\mu_c\right) = -\delta\mu_c$, i.e. the point that jumps immediately to the saddle point. Furthermore, assume the inbound distribution is flat between $\delta\mu_c, f^{-1}\left(\delta\mu_c\right)$. TODO: empirically, $\mu_c \sim \epsilon T$ is *flat* with η, probably just because we're not getting sufficiently close to the saddle point for the $\propto \sqrt{\eta}$ to kick in.

Then, we can compare the empirical Poincaré section of the points that cross the separatrix versus the total predicted interval width $\delta\mu_c, f^{-1}\left(\delta\mu_c\right)$; this would predict 7.2%, 18%. This does alright!

2.5 Consideration 4: Plotting Stable/Unstable manifolds

We can plot the stable/unstable manifolds of two Cassini States as in Fig. 2. Then, since phase space is roughly flat near $\phi = \pi$ (near $\phi = 0$, $\dot{\phi}$ varies drastically and so phase space is "squished" a bit via Liouville's Theorem), we just need to compare the distance between $\mathscr{W}_S^{(0)}$ and $W_U^{(0)}$, the capture gap, to the distance between $\mathscr{W}_S^{(1)}$ and $W_U^{(0)}$ the Melnikov gap, to estimate the capture probability.

The Melnikov gap is predicted above as $d(q^0)$ or approximately

$$\Delta_M \approx \frac{2\pi\epsilon}{\sqrt{4\eta \sin I}}. \tag{13}$$

The capture gap is much trickier to predict, since it depends on the separation between $\mathscr{W}_S^{(0)}$ *after passing through* $\mathrm{CS}_4^{(1)}$. Instead, let's consider the closed orbit in the absence of dissipation that starts at CS4', the modified CS. This orbit has a finite period set by equating $\int_0^T \frac{\partial \phi}{\partial t}\, \mathrm{d}t = \int_0^{2\pi} \mathrm{d}\phi + \int_{2\pi}^0 \mathrm{d}\phi$.

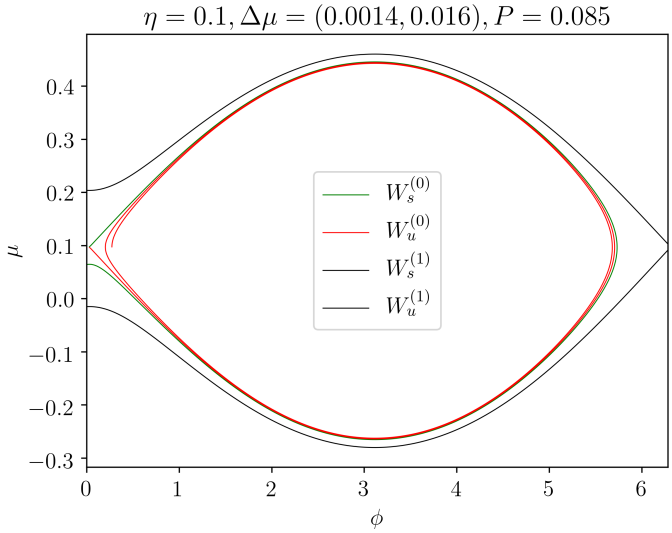

Figure 2: Stable/Unstable manifolds of the two Cassini State 4s.

Now, let's reconsider the Melnikov integral when perturbing this finite (non-homoclinic orbit); this may no longer be an exact result but should give the correct scaling:

$$M_c = \int_0^T \frac{\partial \phi}{\partial t} \epsilon \left(1 - \mu^2\right) \mathrm{d}t. \tag{14}$$

Naively, we might claim that, since $\frac{\partial \phi}{\partial t}$ changes signs halfway through the interval of integration, that the only surviving component is $2\epsilon \bar{\mu} \mu'$, where $\bar{\mu} = \mu_4$ is the average value of μ and μ' is the fluctuation. This gives

$$M_c = 2 \int_0^{2\pi} 2\epsilon \frac{\eta \cos I}{1 + \eta \sin I} \sqrt{2\eta \sin I \left(1 - \cos \phi\right)} \, \mathrm{d}\phi. \tag{15}$$

Note that $M_c \propto \eta^{3/2}$, and since the gap opened $\Delta_c = \frac{M_c}{\frac{\partial \phi}{\partial t}} \propto \eta$, it seems like we're on the right track. Specifically:

$$M_c \approx \epsilon 2\eta \cos I A_{sep}, \tag{16}$$

$$\Delta_c \approx 2\epsilon\eta \cos I \left(16\sqrt{\eta \sin I}\right) \frac{1}{\sqrt{4\eta \sin I}}, \tag{17}$$

$$\approx 16\epsilon\eta \cos I. \tag{18}$$

This also agrees exceedingly well with our simulations This then gives us hopping probability

$$P_{hop} = \frac{\Delta_c}{\Delta_M} \approx \frac{16\eta^{3/2} \cos I \sqrt{\sin I}}{\pi}. \tag{19}$$

This agrees perfectly with the cases we've run.

3 Weak Tidal Friction, changing η

Previously, we took the effect of tides to simply be $\frac{\mathrm{d}\hat{s}}{\mathrm{d}t} = \epsilon \hat{s} \times \left(\hat{l} \times \hat{s}\right)$, but in reality, tides will spin down the body (in our case, planet) at the same rate as aligning $\hat{s}$ to $\hat{l}$. We must treat more carefully.

3.1 Equations of Motion

We first write out the full forms of the EOM without tidal friction. These are taken from Kassandra's Equations 1–3 except I replace subscript $\star$ with subscript s since we are interested in the case where the spin of planet 1 evolves with its coupling to its orbital angular momentum and perturber. We obtain (maybe?)

$$\frac{\mathrm{d}\hat{s}}{\mathrm{d}t} = \omega_{s1}\big(\hat{s}\cdot\hat{l}_1\big)\big(\hat{s}\times\hat{l}_1\big) - \omega_{1p}\cos(I)\big(\hat{s}\times\hat{l}_p\big), \tag{20}$$

$$\omega_{s1} = \frac{3k_q}{2k}\left(\frac{R_1}{a_1}\right)^3 s, \tag{21}$$

$$\omega_{1p} = \frac{3m_p}{4m_1}\left(\frac{a_1}{a_p\big(1-e_p^2\big)}\right)\Omega_1. \tag{22}$$

Note here that s is the spin frequency and $\Omega_1 = \sqrt{GM_1/a_1^3}$ is the Keplerian orbital frequency.

In the presence of tides, and further assuming $s \ll l_1$, we may write (Lai 2012, Equations 43–44, also Ward 1975 Equation 9 & 13)

$$\frac{1}{s}\frac{\mathrm{d}s}{\mathrm{d}t} = \frac{1}{s}\frac{\mathrm{d}s}{\mathrm{d}t} = \frac{1}{t_s}\frac{L}{2S}\left[\cos\theta - \frac{s}{2\Omega_1}\big(1+\cos^2\theta\big)\right], \tag{23}$$

$$\frac{\mathrm{d}\theta}{\mathrm{d}t} = -\frac{1}{t_s}\frac{L}{2S}\sin\theta\left(1 - \frac{s}{2\Omega_1}\cos\theta\right). \tag{24}$$

Note that $L = \mu a^2\Omega_1, S = Is$ are the orbital and spin angular momenta espectively.

It is perhaps easiest to define $\frac{s}{s_c} = \frac{\omega_{s1}}{\omega_{1p}\cos I}$ and $\epsilon\frac{2\Omega_1}{s} = \frac{L}{2St_s\omega_{1p}\cos I}$ while rescaling time $\tau = \omega_{1p}\cos(I)t$, so that we obtain equations of motion

$$\frac{\mathrm{d}\hat{s}}{\mathrm{d}\tau} = \frac{s}{s_c}\big(\hat{s}\cdot\hat{l}_1\big)\big(\hat{s}\times\hat{l}_1\big) - \hat{s}\times\hat{l}_p + \frac{\epsilon 2\Omega_1}{s}\left(1 - \frac{s}{2\Omega_1}\big(\hat{l}_1\cdot\hat{s}\big)\right)\hat{s}\times\big(\hat{l}_1\times\hat{s}\big), \tag{25}$$

$$\frac{\mathrm{d}s}{\mathrm{d}\tau} = \epsilon 2\Omega_1\left(\hat{s}\cdot\hat{l}_1 - \frac{s}{2\Omega_1}\Big(1+\big(\hat{s}\cdot\hat{l}_1\big)^2\Big)\right). \tag{26}$$

s_c has the interpretation of being the critical spin such that the $s1$ coupling is roughly equal strength to the $1p$ coupling. There then seem to be a few outcomes that we might expect:

- Fast evolution towards CS1, then tides will slowly change s without changing $\hat{s}$.
- Fast evolution towards CS2, then tides are strong while state lives inside separatrix maybe? Then will spin down rapidly near CS2 until spin-orbit coupling is weak.
- Slow evolution that trails behind separatrix, expect state to converge somewhere below separatrix? Would probably stay on level curve of high-η H from earlier? Includes anything that doesn't make it to separatrix, including almost fully anti-aligned.

3.2 Crude Analytic Estimate

To make the equations more anemable to analytic analysis (not simulation), let's write down the EOM in (μ,ϕ) coordinates again. The ϕ EOM does not change from the tide-free case, so we can

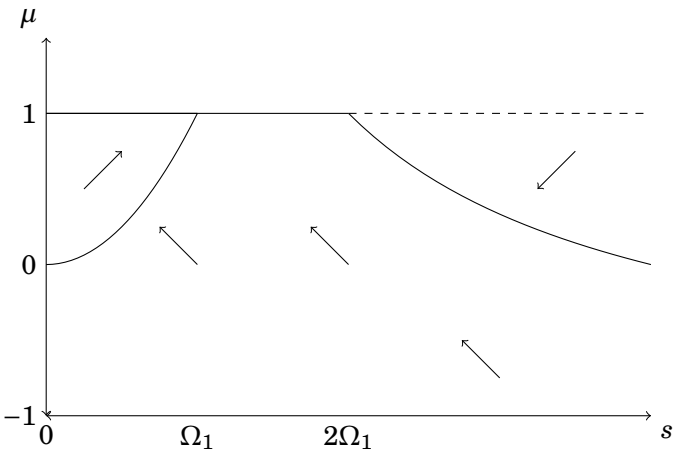

Figure 3: Rough phase portrait of ϕ-averaged equations. Dashed lines indicate unstable zeros of at least one of the EOM, while solid lines indicate stable zeros of at least one of the EOM. The zeros are $\mu = 1$, which becomes unstable at $s = 2\Omega_1$, $s = 2\Omega_1/\mu$ and $s' = 0$. The only fixed point is $\mu = 1, s = \Omega_1$.

reuse earlier equation:

$$\frac{\partial\phi}{\partial\tau} = \frac{s}{s_c}\mu - \left(\cos I + \sin I \frac{\mu}{\sqrt{1-\mu^2}}\cos\phi\right), \tag{27}$$

$$\frac{\partial\mu}{\partial\tau} = -\sin I \sin\phi + \epsilon\frac{2\Omega_1}{s}\left(1-\mu^2\right)\left(1-\frac{s}{2\Omega_1}\mu\right), \tag{28}$$

$$\frac{\mathrm{d}s}{\mathrm{d}\tau} = \epsilon 2\Omega_1\left(\mu - \frac{s}{2\Omega_1}\left(1+\mu^2\right)\right). \tag{29}$$

Assuming $s \gg s_c$ the strong spin-orbit coupling regime, let's first try assuming μ is roughly constant over the course of a precession period, then we can average out the ϕ dependencies. Then ϕ drops out of the EOM, and we have approximate averaged equations

$$\begin{aligned}\frac{\partial\mu}{\partial(\epsilon\tau)} &\approx \frac{2\Omega_1}{s}\left(1-\mu^2\right)\left(1-\frac{s}{2\Omega_1}\mu\right),\\ &\approx \left(1-\mu^2\right)\left(\frac{2\Omega_1}{s}-\mu\right),\end{aligned} \tag{30a}$$

$$\frac{1}{\Omega_1}\frac{\mathrm{d}s}{\mathrm{d}(\epsilon\tau)} \approx 2\mu - \frac{s}{\Omega_1}\left(1+\mu^2\right). \tag{30b}$$

These EOM produce roughly the phase portrait Fig. 3. In the last term, we note $s \gtrsim 2\Omega_1$ initially, while $\mu \leq 1$, so we drop both the linear contribution from μ and approximate $\left(1+\mu^2\right) \approx 1$ so that $\frac{\mathrm{d}(s/\Omega_1)}{\mathrm{d}(\epsilon\tau)} \approx -s/\Omega_1$.

With all these approximations, we clearly obtain $s(\tau) \approx s(0)e^{-\epsilon\tau}$, so the critical synchronization timescale is $\tau_{sync} \sim \frac{1}{\epsilon}$.

3.3 Reaching a Cassini State

As already stated above, the hypothesis is that starting above the separatrix results in obliquity excitation at secular resonance/bifurcation when $\eta = \eta_{crit}$, while starting inside the separatrix probably means the point will stay on CS2 past (saddle-node) bifurcation. We will eventually run numerical simulations to confirm this; we should probably derive modified Cassini states under weak tides to determine exactly where CS1, CS2 lie in this regime.

Finally, if the IC starts below the separatrix, it will evolve to either CS1 or CS2 if it can *catch up* to CS4, else it will stay below the separatrix up until bifurcation and slowly tidally align in the small η limit. Note that CS4 is located at $\mu_4 = \frac{\eta\cos I}{1+\eta\sin I} \approx \frac{s_c}{s}\cos I$, so we can compute $\frac{\mathrm{d}\mu_4}{\mathrm{d}(\epsilon\tau)}$ and compare to $\frac{\mathrm{d}\mu}{\mathrm{d}(\epsilon\tau)}$ in the precession-averaged equations. Thus,

$$\begin{aligned}\frac{\mathrm{d}\mu_4}{\mathrm{d}(\epsilon\tau)} &= -\frac{s_c}{s^2}\cos I\frac{\mathrm{d}s}{\mathrm{d}(\epsilon\tau)},\\ &\approx \frac{s_c}{s}\cos I.\end{aligned}$$

The precession averaged equations bound $\frac{\mathrm{d}\mu}{\mathrm{d}(\epsilon\sigma)} < \frac{2\Omega_1}{s}$, so in order for $\mu < \mu_4$ to approach the Cassini state, we need $\Omega_1 \gtrsim s_c$ by a reasonable margin.

To be more precise, μ_4 disappears at

$$\eta = \eta_c \equiv \left(\sin^{2/3} I + \cos^{2/3} I\right)^{-3/2}. \tag{31}$$

Thus, we can set $s = \frac{s_c}{\eta_c}$ and $\mu = \mu_4$ and integrate backwards Eq. 30 backwards in time to determine μ, s that are exactly sufficient for separatrix crossing. Physically, we never expect $s < \Omega_1$ though, so the minimum s_c we can use and still expect to see a strong spin-orbit coupling regime appear is $s_c \geq \Omega_1\eta_c$.

At the same time though, looking at the phase portrait Fig. 3, we can expect that running backwards in time will easily take us towards the upper right quadrant, where $\mu \to 1$ backwards in time. To start from a misaligned state, the final s_f has a maximum $s_{f,\max}$, and therefore s_c cannot be so large that $s_{f,\max}\eta_c < s_c$, otherwise the bifurcation will arrive before $\frac{\mathrm{d}\mu}{\mathrm{d}t}$ can catch up.

This implies that s_c is bound from both directions in order to get separatrix hopping before the bifurcation disappears.

4 Weak Tidal Friction, Take 2

I did a bunch of work w/o writing it up, so this is the basic gist.

- We can still reuse the same equations as earlier, and the key point to notice is that for a given trajectory, only times $\phi = 0$ are important for determining the final fate of the system. Call these μ_0, then the dynamics of the system can be described by a map $\mu_{0,i+1}(\mu_{0,i}, s)$. The reason μ_0 is important is that only when $\mu_0 = \mu_4(s)$ CS4 can separatrix hopping occur. Thus, whenever μ_0 crosses $\mu_4(s)$, there is some probability of entering the separatrix and some probability of hopping over it.

- The dynamics of the system are then governed by the dynamics of the map near μ_4. In the limit where ϕ is approximately constant over a precession (μ_0 is far from μ_4 compared to $\sqrt{\eta\sin I}$ the separatrix width), then the map obeys nearly the same dynamics as the continuous flow in (μ, s) space for tidal friction.

- However, when we are sufficiently close to μ_4, we enter the $\mu_0 - \mu_4 \lesssim \sqrt{2\eta\sin I}$ regime. Here,

let's note that the map takes on dynamics:

$$\begin{aligned}
\frac{\mathrm{d}\mu_0}{\mathrm{d}t} &= \frac{\partial\mu_0}{\partial H}\frac{\mathrm{d}H}{\mathrm{d}t}, \\
&= \frac{\dot{\phi}}{\dot{\phi}(\phi=0)}\left(\epsilon\left(1-\mu^2\right)\left(\frac{2\Omega_1}{s}-\mu\right)\right), \\
\left\langle\frac{\mathrm{d}\mu_0}{\mathrm{d}t}\right\rangle &= \frac{1}{T}\int_0^T \frac{\dot{\phi}}{\dot{\phi}_0}\epsilon\left(1-\mu^2\right)\left(\frac{2\Omega_1}{s}-\mu\right)\mathrm{d}t, \\
&= \frac{1}{T}\int_0^{2\pi} \frac{1}{\dot{\phi}_0}\epsilon\left(1-\mu^2\right)\left(\frac{2\Omega_1}{s}-\mu\right)\mathrm{d}\phi, \\
&\sim \frac{\sqrt{\eta\cos I}}{2\pi}\frac{1}{\dot{\phi}(\phi=0)}\int_0^{2\pi}\epsilon\left(1-\mu^2\right)\left(\frac{2\Omega_1}{s}-\mu\right)\mathrm{d}\phi. \qquad (32)
\end{aligned}$$

We have substituted $\cos I/2\pi \sim 1/T$ a rough estimate for the period. But now, $\frac{1}{\dot{\phi}(\phi=0)}$ near μ_4 obeys the linearization about the saddle point, and importantly it is small. Near μ_4, the linearization we computed above tells us that $\dot{\phi} \approx -\sin I\Delta\mu$, and so we can imagine the true map dynamics by a flow with $\frac{\mathrm{d}\mu_0}{\mathrm{d}t}$ of form

$$\frac{\mathrm{d}\mu_0}{\mathrm{d}t} = \begin{cases} \frac{\mathrm{d}\mu_0}{\mathrm{d}t} & |\Delta\mu| \gtrsim 2\sqrt{\eta\sin I}, \\ -\frac{\cot I}{2\pi\Delta\mu}\epsilon\left(1-\mu_{eff}^2\right)\left(\frac{2\Omega_1}{s}-\mu_{eff}\right) & \text{otherwise.} \end{cases} \qquad (33)$$

We've defined $\Delta\mu = \mu_0 - \mu_4$ for convenience. μ_{eff} reflects the fact that the ϵ integral in Eq. 32 is taken over a curve of very non-constant μ, roughly following the separatrix boundary. In fact, $\mu_{eff} \sim \sqrt{2\eta\sin I}$ the separatrix width, likely.

Our approximation near μ_4 is probably only accurate up to scaling, we should ensure this piecewise definition is smooth. Thus, we choose $\mu_{eff} \equiv \mu_0 + 2\sqrt{\eta\sin I}$ and change the close-in term to be $\frac{\Delta\mu_{eff}}{\Delta\mu}\left.\frac{\mathrm{d}\mu_0}{\mathrm{d}t}\right|_{\mu_{eff}}$.

We can compare these predictions qualitatively to the actual integrated map. By integrating the true (μ,ϕ,s) system over a period, we can derive an effective $\frac{\Delta\mu}{\Delta t}$ and compare to the scaling we obtain above. The coefficients are not perfect, but the $1/\Delta\mu$ scaling is correct: Fig. 4.

- The thing that is interesting now is that μ_{eff} is evaluated relatively farther away from μ_4, and since $\frac{\mathrm{d}\mu}{\mathrm{d}t}$ in the weak tidal limit for $s > 2$ can be negative, it is possible for a point above μ_4 to be *sucked in* to CS4 *from both above and below*. This is an extremely important feature, and indeed in Fig. 4 we see such behavior. If we are in this regime, then any nonzero separatrix hopping probability will drive 100% of points incident on CS4 to enter the separatrix, since repeated hoppings must be observed!

  Qualitatively, we can use our piecewise definition to see the behavior of this transition; it occurs when $\frac{\mathrm{d}\mu}{\mathrm{d}t}$ evaulated at the μ_{eff} above μ_4 is negative, i.e. above $\frac{2\Omega_1}{s}$. Thus, this boils down to $\mu_4 + 2\sqrt{\eta\sin I} \gtrsim \frac{2\Omega_1}{s}$. Since $\mu_4 \approx \eta\cos I = \frac{s_c\cos I}{s}$, we see that for smaller s_c than some critical threshold, μ_4 is no longer attracting on both sides. We can numerically solve for this transition using the full integrated equations: Fig. 5.

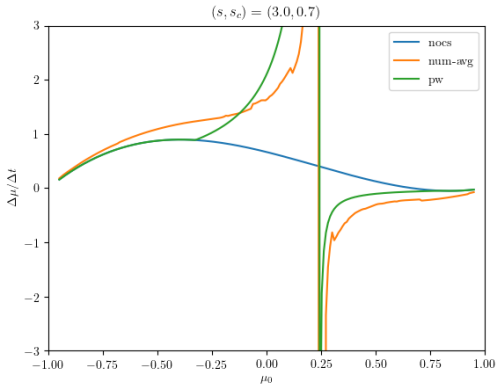

(a) $\frac{\Delta\mu}{\Delta t}$ computed using the pure weak tide prescription (ignoring $\mu(\phi)$ variations), computed using an integral of the full system and computed using the piecewise definition above.

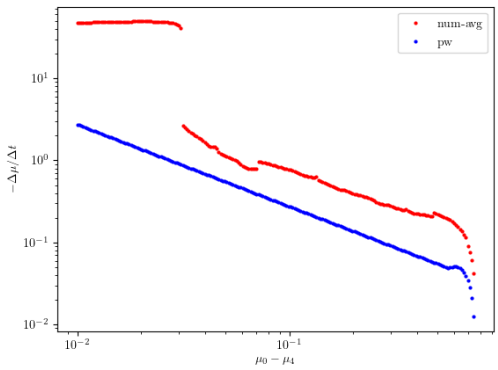

(b) Loglog plot of $\Delta\mu/\Delta t$ above μ_4 for the integrated and piecewise solutions.

Figure 4: Agreement of piecewise with integrated, qualitatively.

- Indeed, Fig. 5 shows that the critical s_c is a fairly flat function of s in our parameter regime of interest. Call this critical s_c S_0 owing to unfortunate notation. We can thus identify two regimes:
  - $s_c < S_0$: points above CS4 will be driven away from CS4, and so only points below the separatrix will experience a single chance to separatrix hop. Thus, in this regime, points initially above the separatrix will tidally synchronize, while points below the separatrix will probabilistically either synchronize or go to CS2.
  - $s_c > S_0$: CS4 becomes *attracting*, and so two consequences: points initially above the separatrix are sucked downwards, and all encounters go to CS2 after 100% separatrix entry probability.

  Since S_0 is some function of s, it is clear that for intermediate values of s_C, we will see single separatrix hopping at early times while separatrix attraction at late times.

- Finally, we may compare histograms of outcomes when $s_c > S_0, s_c < S_0$. For $s_c > S_0$, all points get attracted into CS2, which then synchronizes quickly; this is illustrated poorly in Fig. 6a.

  On the other hand, when $s_c < S_0$, points below CS4 only get one chance at hopping. We can perform similar Melnikov calculation to above by integrating the true tidal term $\frac{\partial\mu^{(1)}}{\partial t} = \epsilon(1-\mu^2)(2\Omega_1/s - \mu)$ and find that the hopping probability $P_{hop} \propto \frac{\mu}{2\Omega_1/s} \propto \sqrt{s}$ or in fact scaling with $\eta^{-1/2}$; the difference comes in the $1/s$ dependence in the single-leg integral and the $-\mu$ factor in the double-leg integral. Thus, points closer to the initial separatrix actually should experience higher entry probability, also observed in Fig. 6b.

  Finally, we can somewhat see what the transition regime looks like in Fig. 6c. Points close to the separatrix experience attracting dynamics and all hop, while points far away from the separatrix experience the $\sqrt{s}$ hopping probability.

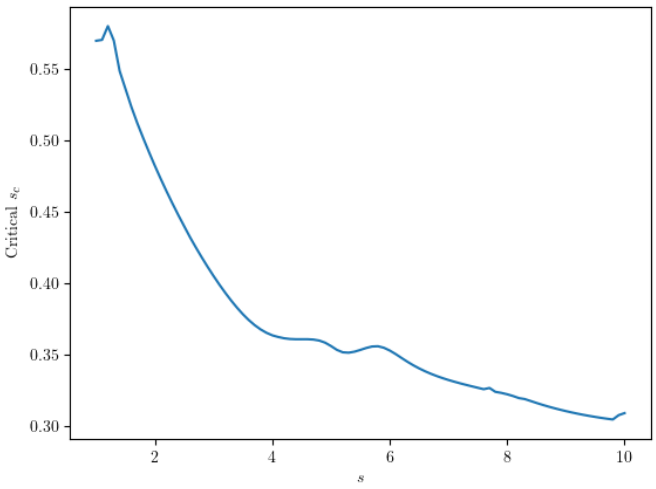

Figure 5: Critical values of s_c below which μ_4 is no longer strongly attracting.

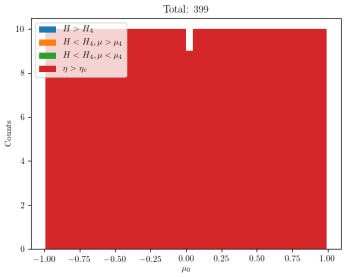

(a) Outcomes when $s_c = 0.7 > S_0$.

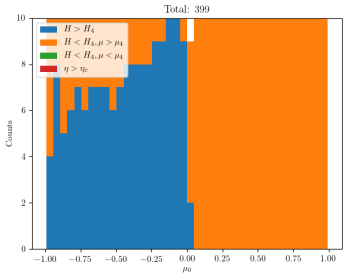

(b) Outcomes when $s_c = 0.2 > S_0$.

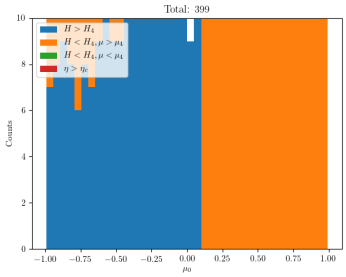

(c) Outcomes when $s_c = 0.3 \sim S_0$.

Figure 6: Outcome hists.